Polymerization of human angiotensinogen: insights into its structural mechanism and functional significance

Peter Stanley, Louise C Serpell, Penelope E Stein

Biochemical Journal Immediate Publication. Published on 27 Jul 2006 as manuscript BJ20060444

Polymerization of human angiotensinogen: insights into its structural mechanism and functional significance

Peter STANLEY*, Louise C. SERPELL † and Penelope E. STEIN * [1]

* Division of Structural Medicine, Department of Haematology, Cambridge Institute for Medical Research, Wellcome Trust/MRC Building, Cambridge, CB2 2XY, United Kingdom, and † Dept. of Biochemistry, School of Life Sciences, University of Sussex, Falmer, E. Sussex.

Running Title: Angiotensinogen Polymers

This study was supported by the Wellcome Trust (Grant 054518/Z/98/Z).

[1] To whom correspondence should be addressed (telephone. 44 1223 762660. fax: 44 1223 336827. email: pes1000@cam.ac.uk)

Biochemical Journal Immediate Publication. Published on 27 Jul 2006 as manuscript BJ20060444

We have studied the *in vitro* polymerization of human plasma angiotensinogen (AGT), a noninhibitory member of the SERine Protease INhibitor (serpin) family. Polymerization of AGT is thought to contribute to a high molecular weight form of the protein in plasma that is increased in pregnancy and pregnancy-associated hypertension. Our results show that the polymerization of AGT occurs through a novel mechanism which is primarily dependent on noncovalent linkages, while additional disulphide linkages formed after prolonged incubation are not essential for either formation or stability of polymers. We present the first analyses of AGT polymers by electron microscopy, CD spectroscopy, stability assays and sensitivity to proteinases and we conclude that their structure differs from the "loop-sheet" polymers typical of inhibitory serpins. Histidines within the unique N-terminal extension of AGT appear to influence polymer formation, although it can still take place after their removal by renin. At a functional level, we show that AGT polymers are not substrates for renin, so polymerization of AGT in plasma would predictably lead to decreased formation of AngI with blood pressure lowering. Polymerization may be therefore an appropriate response to hypertension. The ability of AGT to protect its renin cleavage site through polymerization may explain why the AngI decapeptide has remained linked to the large and apparently inactive serpin body through evolution.

Key words: angiotensinogen, serpin, polymers, renin, noninhibitory, hypertension.

INTRODUCTION

Angiotensinogen (AGT) is a 452 amino acid glycoprotein which is a member of the SERine Protease INhibitor (serpin) family of proteins [1,2], showing sequence identities of 25% or less with other plasma serpins and containing a unique 50 residue N-terminal extension. AGT appears to have evolved a noninhibitory function and has not been found to inhibit any proteinase. In common with at least three other noninhibitory serpins (ovalbumin, pigment epithelial-derived factor and maspin) [3-5] AGT does not undergo the stressed-relaxed conformational change that characterizes inhibitory members of the family [3].

AGT has a unique role among serpins acting as a precursor for angiotensin peptides. In the initial rate-limiting step of the renin-angiotensin system (RAS), the aspartyl proteinase renin cleaves AGT at its N-terminus, generating the inactive decapeptide angiotensin I (AngI) and leaving the remaining 98% of the molecule as a much larger fragment called des(AngI)AGT. AngI is further hydrolyzed by angiotensin converting enzyme to give the active octapeptide angiotensin II, which regulates blood pressure, salt and water homeostasis, and vascular tone [6,7]. Linkage studies strongly implicate the AGT gene in the pathogenesis of essential hypertension [8].

Human plasma AGT is a heterogeneous protein which migrates on SDS-polyacrylamide gel electrophoresis (SDS-PAGE) as two bands of approximately 60 kDa. Glycosylation accounts for up to 14% of its molecular mass and plays a predominant role in its heterogeneity [9,10]. In addition to monomeric AGT, a small portion of the circulating AGT has a higher mass and is referred to as high molecular weight AGT (HMrA) [11]. Around 3% of the AGT in plasma from normotensive, nonpregnant individuals comprises HMrA. However, the first half of pregnancy is associated with a 4-fold increase in total AGT and 20-fold increase in HMrA in plasma. The proportion of HMrA can reach as high as 28% in pregnancy-associated hypertension [12,13]. HMrA is the major form of AGT in amniotic fluid and in the placenta [14] where it can comprise up to 80% of the total AGT.

One component of HMrA is composed of disulphide-linked complexes with the proform of eosinophil major basic protein [15]. However, these complexes differ from the major form of HMrA in plasma and placental tissue which is composed of polymers of monomeric AGT held together by noncovalent and disulphide bonds [16-18]. In addition, most of the

placental HMrA is cleaved in the part of the sequence homologous to the reactive centre loop (RCL) of an inhibitory serpin [19,20].

Two particular areas of contention in the current literature are addressed in this work. The first concerns the nature of the bonds that hold AGT polymers together. Many inhibitory members of the serpin family can form polymers through a "loop-sheet" interaction between the RCL of one molecule and the main β-sheet of another, and this noncovalent mechanism has been proposed to explain the formation of HMrA [18,20], while another theory suggests that disulphide linkages play the predominant role in the formation of HMrA [21]. The second area of contention concerns the ability of AGT polymers to act as a substrate for renin. Early work on HMrA isolated from plasma concludes that it is recognized by renin [22,23]. However, later work with purified recombinant protein suggests that AGT aggregates are not recognised by renin, possibly due to the presence of intermolecular disulphide bridges [21].

Here we describe a study of the polymerization of AGT using an established *in vitro* system which can replicate the size distribution, nature of the polymer linkages, and state of the RCL found in *ex vivo* polymers isolated from plasma and placental tissue. We find that the properties of AGT polymers fit neither of the previously reported models and present an alternative mechanism for polymerization. Our findings of the structural nature of AGT polymers serve as a starting point towards understanding their physiological significance.

EXPERIMENTAL

Materials

Unless otherwise stated all reagents were purchased from Sigma (Dorset, UK). Human recombinant renin was a gift from D. Thibeault (Roche, Canada), and α1-antitrypsin was from Athens Research and Technology (Athens, GA). Chromatography media were from Amersham Biosciences (Blue Sepharose 6 FF, DEAE Sepharose FF, Superdex S200 and Superose 12), BioRad (ceramic hydroxyapatite) and Applied Biosystems (POROS 20 PI). Polyacrylamide gel protein markers were from Bio-Rad. Polyclonal antibody to AGT was a gift from D. Tewksbury (Marshfield Medical Research Foundation, USA) and the AngI polyclonal antibody was purchased from Cambio (Cambridge, UK). A synthetic peptide

corresponding to the P14-P3 sequence of antithrombin (acetyl-SEAAASTAVVIA) was supplied by MWB (Cambridge, UK).

Purification of human AGT

Native AGT was purified from fresh human plasma by 1.4 M and 2.4 M ammonium sulphate fractionation followed by the four chromatography steps described by Tewksbury [24]**:** 1. Blue Sepharose 6 FF; 2. DEAE Sepharose FF; 3. Ceramic Hydroxyapatite; and 4. POROS 20 PI. A final gel filtration step on Sephacryl S200 separated the monomeric form of AGT from *ex vivo* polymers. AGT was stored at 4 ^{o}C. Its concentration was determined by UV absorbance at 280 nm using an extinction coefficient (1 mg/ml) of 0.92. Typically, 2.5 mg of monomeric AGT could be purified from 250 ml plasma with a yield of more than 15%. AGT was identified by its immunoreactivity against α−AGT antibody and its purity was assessed by SDS- and nondenaturing-PAGE. Monomeric protein migrated as a doublet band on both types of gel. Both bands were confirmed to be intact AGT by N-terminal sequencing (1DRVYI) and matrix-assisted laser desorption ionization-time of flight mass spectrometry (MALDI-TOF) of derived tryptic peptides. N-terminal sequencing was performed by the Protein and Nucleic Acid Chemistry facility of the Department of Biochemistry, University of Cambridge, and MALDI-TOF by the Proteomics Facility of the MRC Dunn Human Nutrition Unit, Cambridge.

Polymerization of AGT

Native AGT in buffer (0.07 - 5.0 mg/ml) was incubated between 37 to 55 ^{o}C for durations up to 70 days. Polymerization was assessed on nondenaturing and SDS-PAGE gels and the proteins were visualized by staining with silver (Bio-Rad Silver Stain Plus) or with Coomassie Blue. Residual monomeric protein was quantified by densitometry of stained gels using Quantity One software (Bio-Rad).

To determine the pH dependence of AGT polymerization, samples of AGT were buffer exchanged to 10 mM sodium phosphate, 150 mM NaCl, 1.0 mM EDTA, pH 7.4 and concentrated to 2.0 mg/ml in a 30k cut-off spin concentrator (Vivascience). 2 μl aliquots were diluted 10-fold into 50 mM sodium phosphate, 150 mM NaCl, 0.5 mM EDTA at pH 4.0 to 9.0 and incubated at room temperature for 1 h. Samples (0.2 mg/ml) were then heated at 55 ^{o}C for 1 h and run on nondenaturing gels to assess the extent of polymerization.

Chemical modification of AGT

Stock solutions of dithiothreitol (DTT) in water and N-ethylmaleimide (NEM) in absolute ethanol were freshly prepared. Native AGT (1.0 mg/ml) in 20 mM sodium phosphate, 75 mM NaCl, 1.0 mM EDTA, pH 7.0 was incubated with 10 mM DTT or NEM in a volume of 50 μl at 25 °C for 2 h. The reduced and alkylated forms of AGT were then diluted 5-fold in buffer and incubated for 54 h at 4 °C or 55 °C.

Stock solutions of DEPC were freshly prepared in absolute ethanol. Native AGT (1.0 mg/ml) in 20 mM sodium phosphate, 75 mM NaCl, 1.0 mM EDTA, pH 6.0 was incubated with 1.0 mM DEPC in a volume of 50 μl at 25 °C for 15 min. The reaction was quenched with 5.0 mM imidazole. As a control, an equivalent volume of absolute ethanol (minus DEPC) was added to a parallel mixture and treated identically.

Preparation of reactive centre -cleaved and N-terminal – cleaved forms of AGT

To prepare reactive centre loop-cleaved AGT, native AGT (0.5 mg/ml) was incubated with thermolysin (50 μg/ml) at a final protein: proteinase ratio of 200:1 (w/w) in 20 mM Tris-Cl, 150 mM NaCl, 2 mM $CaCl_2$, pH 7.0 at 37 °C for 60 min and the reaction stopped by the addition of EDTA to 10 mM. Cleavage was confirmed by SDS-PAGE, mass spectroscopy, and N-terminal sequencing of the products. Cleaved AGT was buffer exchanged and purified by gel filtration on Superose 12.

Large scale N-terminal cleavage of AGT (200 μg; 0.2 mg/ml) by recombinant human renin (3.0 nM) was performed at 37 °C in 30 mM sodium phosphate, 150 mM NaCl, 1 mM EDTA, pH 6.0. After 72 h, completion was confirmed by the lack of immunoreactivity against an α-AngI antibody. Des(AngI)AGT was buffer exchanged to pH 7.4, separated from AngI and other products by gel filtration on Superose 12, and concentrated in a spin concentrator.

Accessibility of the reactive centre loop in AGT polymers

Native AGT (0.4 mg/ml) was either heated at 55 °C for 54 h to form polymers or stored at 4 °C as the monomeric form. The presence of polymers in the heated sample was confirmed by nondenaturing PAGE, followed by addition of $CaCl_2$ to 2.5 mM. 5 μg aliquots of native

and polymer forms were incubated with thermolysin at protein: proteinase ratios up to 250:1 (w/w) at 37 °C for 60 min. Reactions were stopped by placing on ice and adding EDTA to 10 mM.

Renin cleavage of monomeric and polymeric AGT

Native AGT (0.15 mg/ml) in buffer was heated at 55 °C for up to 18 h. Aliquots were removed at intervals and run on gels to confirm the extent of polymerization. Further aliquots (2 μg) were removed, diluted with an equal volume of 3.0 nM renin in physiological buffer (pH 7.4) and incubated at 37 °C for 1 h. Reactions were stopped by the addition of reducing SDS-PAGE loading buffer and snap-frozen in liquid nitrogen.

Native AGT and RCL cleaved AGT (0.3 mg/ml) were heated at 55 °C for 2 h or stored at 4 °C. Aliquots were removed and run on gels to confirm the extent of polymerization. Further aliquots (10 μg) were removed, diluted with an equal volume of 1.0 nM renin in physiological buffer (pH 7.4), and incubated at 37 °C for intervals up to 8 h. The reactions were stopped as above. Aliquots were run on duplicate SDS-PAGE gels, and transferred to PVDF membrane for Western blot analysis with α-AGT and α-AngI antibodies.

Polyacrylamide gel electrophoresis and immunoblotting

The discontinuous system of Schagger and von Jagow [25] was used for SDS-PAGE. For nondenaturing polyacrylamide gel electrophoresis, gels were cast with 0 to 8 M urea and run with 70 mM Tris, 190 mM glycine, pH 8.8. AGT was electrotransferred to Immobilin-P PVDF (Millipore) and the membranes blocked in 10 % (w/v) dried milk [26]. AGT was detected with rabbit antiserum against AGT (at 1/ 15 000 dilution) and revealed with goat anti-rabbit IgG conjugated to horseradish peroxidase on the addition of ECL substrate (Amersham Biosciences). For sequence analysis, AGT was transferred to P^{SQ} PVDF membranes and stained with 0.1 % (w/v) Amido black/ 20% (v/v) methanol.

Circular dichroism

Circular dichroism (CD) spectra were recorded between 190 and 250 nm on a Jasco J-810 spectropolarimeter with 0.3 mg/ml protein in 10 mM sodium phosphate, 50 mM NaCl buffer (pH 7.4) using a 0.2 mm path length quartz cuvette thermostatically controlled at 25 °C. Each spectrum represents the accumulation of ten scans. Thermal denaturation was

followed by monitoring the CD signal at 222 nm between 25 and 95 °C using a heating rate of 1 °C /min. Melting points (T*m*) were calculated using an expression for a two state transition as described previously [27]. The results are the average of three experiments.

Electron microscopy

Samples for electron microscopy were prepared by incubating native AGT (0.5 mg/ml) in 10 mM sodium phosphate, 50 mM NaCl, pH 7.4 at 55 °C for 24 h. A 4 µl drop was placed onto a carbon-coated grid for 2 min. The grid was blotted, washed with water, negatively stained with 2 % (w/v) uranyl acetate, and air-dried. The grid was examined in a Hitachi 7100 transmission electron microscope at 80 kV. Images were recorded at magnifications of 3–60 k with a Gatan Multi-Scan 794 CCD camera using DigitalMicrograph 3.4.4 software. Image processing was done with Adobe PhotoShop 6.0 software. Individual molecules were visualized at 57,000-fold magnification with photographic enlargement.

RESULTS

Formation and properties of angiotensinogen polymers

Incubation of monomeric AGT at physiological temperature and in physiological buffer at concentrations comparable to those in plasma for periods up to 10 weeks produced discrete high molecular mass ladders of dimers, trimers and higher order polymers (Figure 1(i)). This process was assisted by mild denaturation either by incubation with urea at low temperature (Figure 1(ii)) or by higher temperatures (Figure 1 (iii)).

Monomeric AGT incubated at 55 °C rapidly formed polymers which co-migrated with unheated *ex vivo* AGT polymers isolated from plasma (Figure 1(iii)). Nondenaturing gels showed polymer formation after 5 min, with the order of polymers increasing after longer incubation times, and almost no monomer remaining by 6 h (Figure 2A(i)). The initial polymers dissociated back to the monomer totally on nonreducing SDS-PAGE (Figure 2A(ii)) but after 2 h polymers were visible on nonreducing SDS-PAGE which only dissociated to the monomer after reduction (not shown). After 54 h incubation, AGT formed higher order polymers that were stacked to the top of both types of gel.

Formation of polymers on heating RCL-cleaved AGT

Out of a panel of proteinases, only thermolysin was found to cleave the RCL of AGT at the P6-P5 (412Q, 413L) position, matching the cleavage site found in HMrA isolated from

placental tissue. Cleavage with thermolysin reduced the size of both 60 and 56 kDa AGT bands with generation of a 4 kDa peptide (Figure 2B(i)). The observed mass of the peptide (m/z = 4414.0) matched the calculated mass (Mr = 4414.1) of the C-terminal sequence Leu413 to Ala 452, the last residue of mature AGT. N-terminal sequencing of the peptide confirmed the primary cleavage site at P6-P5 within the RCL. Native AGT was easily distinguished from the RCL-cleaved protein on SDS-PAGE but not on nondenaturing gels (Figure 2B(ii)). The effect of RCL cleavage on the polymerization of AGT was determined by heating thermolysin cleaved AGT at 55 ^{o}C for up to 54 h (Figure 2B(ii) and (iii)). RCL-cleaved AGT retained the ability to polymerize with identical kinetics to those of intact AGT (Figure 2A).

Electron microscopy

Polymers were examined by electron microscopy to confirm that the multimers seen on polyacrylamide gels were ordered polymers and not disordered aggregates. This revealed the presence of mostly linear species, similar to those observed with α1-antitrypsin (Figure 2C(i)). The majority of the filaments were less than 50 nm in length; however, some longer filaments extended to over 100 nm (Figure 2C(ii)).

Kinetic analysis of AGT polymerization

AGT formed polymers when incubated at 48 ^{o}C for 22 h at concentrations between 0.07 and 0.7 mg/ml with loss of monomeric AGT (Figure 3A). The extent of polymerization was assessed by quantification of the monomeric AGT on nondenaturing gels. The decreases in monomer were linear when fitted to a reciprocal plot against time indicating that this was a second order reaction. The overall second order rate constant from a double logarithmic plot of initial velocity against AGT concentration was 3.25 $\pm$ 0.63 L mole^{-1} sec^{-1}.

The effect of thiol group modifications on the ability of AGT to polymerize

Comparison of the amounts of monomeric AGT remaining on nondenaturing and SDS-PAGE gels after heat induced polymerization provides an indication of the relative contributions of noncovalent and covalent linkages (Figure 3B). Covalent linkages were not significant until after 6 h when total polymerization was virtually complete, implying that nearly all polymerization before 6 h was due to noncovalent linkages.

Free cysteine residues of AGT were modified with NEM or DTT prior to heat-induced polymerization to investigate the contribution of disulphide bonding. Nondenaturing PAGE analysis of the products showed a ladder of multimer species totally independent of the state of the cysteine residues (Figure 3C(i)) while nonreducing SDS-PAGE showed complete absence of the normal ladder of disulphide-linked polymers after cysteine reduction or alkylation (Figure 3C(ii)). When pre-polymerized AGT was reduced with DTT, the modified protein still appeared as a polymer on nondenaturing PAGE. Moreover, the size distribution of the polymers was unaltered suggesting that the disulphide bridges linked adjacent monomers in the same strand and not separate polymers (not shown).

Circular dichroism signal changes during the polymerization of AGT

Circular dichroism (CD) was used to study structural changes during AGT polymerization (Figure 4). The far-UV CD spectrum of native AGT monomers indicated the usual presence of both α-helix and β-sheet in a folded protein. However, the presence of a double minimum at 208 nm and 220 nm (Figure 4A) differed from the CD spectra of typical inhibitory serpins at pH 7.4 [28]. The far-UV CD spectrum of cleaved AGT monomers was identical to that of intact AGT (Figure 4A) confirming that RCL cleavage was not accompanied by significant conformational change.

The effect of polymerization on the far-UV CD spectrum of AGT was identical for intact and cleaved AGT. Figure 4B shows an overall 20% reduction in the negative CD signal between 200-240 nm on heating. In addition, the overall shape of the CD spectrum after polymerization differed from that obtained for monomers. Instead of the broad level minimum between 208 and 220 nm there was a single minimum at 215 nm. This pattern differs from the CD spectra of typical inhibitory serpin polymers.The stability of monomeric and polymeric AGT was assessed by monitoring the change in CD signal at 222 nm while increasing the temperature. Figure 5A shows the melting curve for monomeric intact AGT with a calculated T*m* of 60.6 (± 0.3) ºC, similar to typical inhibitory serpins. Thermolysin-cleaved AGT showed an almost identical heat stability profile (T*m* = 59.8 (± 0.4) ºC (not shown)). For polymeric AGT, the change in the 222 nm signal with temperature was far less marked, not decreasing at all below 80 ºC (Figure 5A).

Characterisation of the unfolding of AGT on urea gels

The stabilities of monomeric and polymeric AGT were compared on nondenaturing gels containing 0 to 8 M urea. Monomeric AGT unfolded with a profile similar to that of inhibitory serpins with an unfolding transition at ~4 M urea (Figure 5B). The monomer was stable below 2 M urea and fully unfolded above 6 M urea with a dynamic region in between. AGT polymers unfolded in an identical manner to the monomer with a transition at ~4 M urea and becoming fully unfolded and running as a tight band in 8 M urea. Faint higher molecular weight bands were visible in 8 M urea and presumably represented the small proportion of covalently linked monomers.

Proteolytic cleavage of the reactive centre loop in premade AGT polymers

Susceptibility of the RCL of native and polymerized AGT to cleavage by thermolysin was compared. Cleavage of native AGT yields a 4 kDa peptide and major fragments of 56 and 52 kDa (Figure 6(i)). Cleavage of polymerized AGT showed an identical pattern on SDS-PAGE (Figure 6(i)), confirming that the sites of interaction with thermolysin do not become hidden or disrupted in the polymers. Furthermore, cleavage of the RCL in AGT polymers was not associated with dissociation of the polymeric structure (Figure 6(ii)).

The effect of pH on AGT polymerization

Polymerization of AGT was assessed after incubation at pH 4 to 9. The formation of polymers was insignificant below pH 6.0 and most marked above pH 7.0 (Figure 7A), suggesting that polymerization might depend on the protonation of a histidine residue. Treatment of monomeric AGT with DEPC allowed substantial polymerization under neutral and acidic conditions, with no monomer remaining at any pH value tested (Figure 7B). There are three histidine residues between the AGT N-terminus and the disulphide linkage which connects Cys18 to Cys138 on the serpin body [29]. The effect of breaking this disulphide bridge was tested. AGT that had been reduced with DTT prior to heating was found to polymerize with the formation of noncovalent linkages at pH 7.4, in exactly the same way as intact AGT, although covalent linkages were totally absent (Figure 3B). Moreover, reduced AGT polymerized under neutral conditions similarly to DEPC modified AGT (Figure 7C). The influence of AngI, which includes two histidine residues (His6 and His9), on polymerization was assessed by heating des(AngI)AGT. Renin cleavage of AGT had no effect on polymerization at physiological pH: des(AngI)AGT formed polymers

through noncovalent and disulphide linkages, exactly as intact AGT (not shown). However, des(AngI)AGT also polymerized at pH 7.0 and below (Figure 7D).

Effect of AGT polymerization on Angiotensin I generation

The effect of polymerization on the ability of renin to cleave the N-terminus of AGT was investigated. Monomeric AGT was polymerized at 55 °C for periods up to 18 h. Aliquots were withdrawn, hydrolysed with renin, and run on reducing SDS-PAGE and immunoblotted. The release of the N-terminal AngI decapeptide was followed by loss of reactivity against an α-AngI antibody, with total AGT assessed with an α-AGT antibody. Prior polymerization of AGT proportionally reduced its ability to be cleaved by renin (Figure 8A). This loss in substrate behaviour was essentially complete after 2 h (Figure 2A). However, even after incubation at 55 °C for 54 h, AGT polymers never became fully resistant to renin and a small loss of AngI remained detectable (not shown).

Monomeric intact AGT and thermolysin cleaved AGT were treated at 55 °C for 2 h to produce polymers without significant disulphide bridging prior to incubation with renin for up to 8 h. RCL cleavage was found to make no difference to the response of monomeric or polymeric AGT to renin (Figure 8B). The monomeric AGT samples released AngI at equivalent rates over 8 h. However, after an initial loss of AngI, both intact and RCL-cleaved polymers were totally resistant to further renin hydrolysis.

DISCUSSION

Under physiological conditions, typical inhibitory serpins exist in a metastable state and require partial unfolding by chemical denaturants or heating just below their melting temperatures to induce polymerization. AGT, like other noninhibitory serpins, does not have a metastable native conformation, but we show here that it can polymerize under conditions similar to those which induce polymerization of inhibitory serpins (Figure 1). These *in vitro* AGT polymers were found to be similar to the AGT multimers in HMrA isolated from human plasma and placental tissue which have been previously characterized with masses ranging from 200-550 kDa [17,18,20]. In addition, electron microscopy of *in vitro* AGT polymers revealed bead-like, linear chains of molecules (Figure 2C) similar to polymers formed *in vivo* by inhibitory serpins [30,31], as well as polymers formed *in vitro* at elevated temperatures [32,33]. This suggests that the increase in mass of AGT was due to

the formation of dimers, trimers and higher order polymers rather than nonspecific aggregation.

Loop-sheet polymerization of serpins through s4A and s7A linkages proceeds through two steps: a fast unimolecular phase independent of protein concentration consistent with a conformational change within the monomer, and a slow bimolecular phase dependent on protein concentration representing the formation of polymers. Both phases have been described by first order rate constants [27,34]. Our experiments at 48 ^{o}C with nondenaturing gels measured the rate-limiting production of polymer and did not report on the fast phase (Figure 3A). Velocities derived from the loss of monomer were dependent on protein concentration and defined polymerization as a second order reaction. The second order rate constant of 3.25 L mole^{-1} sec^{-1} expressed as a range of first order constants (0.5 – 5.0 x 10^{-5} sec^{-1}) showed that the rates of AGT polymerization were comparable to those for the slow phases of other wildtype serpins [27,34,35].

The polymerization of AGT was slower at physiological temperature but detectable over several weeks (Fig 1(i)), a rate that was nevertheless probably sufficient to explain the low levels of polymerized AGT found in the circulating plasma of normotensive, nonpregnant individuals. Within the range 0.07 - 0.7 mg /ml AGT polymerization was dependent on the square of the concentration, so that a four-fold increase in AGT would increase the velocity of polymerization 16-fold. Interestingly, a four-fold increase in total AGT over the same concentration range in the first half of pregnancy is associated with a 20-fold increase in HMrA [12,13].

Ex vivo HMrA is held together by both noncovalent bonds and disulphide bonds [18-20] and our results suggest that *in vitro* AGT polymers were stabilized in the same way (Figures 2A and B). We found that the formation of the SDS-sensitive noncovalent linkages and the intermolecular disulphide linkages were temporally separated during polymerization (Figure 3B), with noncovalent bonds forming first as the most important linkage, followed by later disulphide linkages. Indeed, polymerization still occurred in the absence of disulphide linkage (Figure 3C). Furthermore, if pre-made polymers were reduced with DTT, there was no difference in the size distribution of the polymers (not shown).

Presumably, disulphide linkages were formed between adjacent monomers on the same strand rather than between separate polymer strands.

We considered the possibility that AGT polymers possessed the same type of noncovalent linkage as polymers of inhibitory serpins. Polymerization of inhibitory serpins typically involves the intact RCL from one monomer inserting into the A-β-sheet of another monomer in the strand 4A position that it would normally occupy during proteinase inhibition [36]. AGT polymerization was unlikely to involve this A-sheet mechanism since there is good evidence that the RCL of AGT cannot insert into β-sheet A due, firstly, to bulky side chains in the hinge region (P10-P12) of the RCL that would prevent loop insertion [3], and secondly, to sequence features in the A-sheet that would prevent sheet opening [37]. In addition, in this work we have shown that both RCL-cleaved and intact AGT polymerized in the same way on heating (Figure 2A,B), suggesting that polymerization did not involve the RCL. Furthermore, AGT polymers displayed a far-UV CD minimum at 215 nm (Figure 4B) while typical A-sheet polymers retain the single 222 nm trough of the monomer [27]. We also found that AGT polymers did not have the enhanced stability characteristic of typical serpin A-sheet polymers (Figure 5B) [38].

In contrast to A-sheet polymers where the inserted P8-P3 sequence of the RCL is inaccessible [36,39], the P6-P5 position of the RCL of AGT remained exposed after polymerization (Figure 6A(i)). Moreover, cleavage of the RCL of polymers did not disrupt their structure (Figure 6A(ii). Accessibility of the RCL was also inconsistent with other polymer models which involve linkages of the RCL with β-sheet C or the edge of sheet A [35,40-43]. The formation of a stable binary complex between a serpin and an exogenous peptide corresponding to its RCL has been used as a marker of the accessibility of its A-β-sheet [32,44]. A peptide corresponding to the wildtype sequence of the AGT RCL fails to insert in the AGT A-β-sheet [18], suggesting that its A-sheet cannot open. We confirmed this finding using a peptide corresponding to the RCL of antithrombin which has been found to insert in the A-sheet of many different serpins (not shown).

An unexpected finding was that AGT polymerization was dependent on pH (Figure 7A). Involvement of histidine residues (pKa 6.0) was confirmed by DEPC modification which allowed polymerization under acidic conditions (Figure 7B). Furthermore, demodification

by hydroxylamine led to nearly complete recovery of the inhibition of polymerization at pH 6.0 (not shown). Involvement of N-terminal histidine residues was supported by our findings that AGT could be induced to polymerize under acidic conditions by either reducing the disulphide bridge to allow the N-terminus to move from its original position (Figure 7C), or by removal of the AngI peptide with renin (Figure 7D). However, the presence of the N-terminus was not essential for polymerization since des(AngI)AGT produced polymers at physiological pH in the same way as intact AGT (not shown). A mechanism to distinguish between active AGT and inactive des(AngI)AGT would be a desirable component of the RAS. While active AGT does not polymerize significantly below physiological pH, des(AngI) AGT can form polymers at pH 7.0 (Figure 7A and D). This might allow discrimination of the two forms under conditions of mild acidosis, for instance at sites of inflammation [45] or within intracellular compartments [46].

The effect of AGT polymerization on its role as a renin substrate was investigated under physiological conditions of pH, ionic strength, temperature and AGT concentration, following the reaction by directly assaying the loss of AngI from the body of the serpin. Our results showed progressive inaccessibility of the N-terminus of AGT to renin with associated failure of the polymer to act as an efficient renin substrate (Figure 8A). Resistance to renin was proportional to the formation of noncovalent polymers and not disulphide linkages. Recognition of monomeric AGT by renin was unaffected by the state of its RCL (Figure 8B) consistent with the lack of any significant structural changes associated with RCL cleavage. RCL-cleaved and RCL-intact polymers were equally unable to act as renin substrates although this was not clear until the later stages of the reaction when the polymers became resistant to further loss of AngI (Figure 8B). The initial 15% loss in AngI was too great to be explained by residual monomer and may reflect the hydrolysis of the N-termini of AGT molecules at the ends of polymer chains.

Our results strongly exclude the involvement of the reactive centre loop and an open A-sheet in the formation of AGT polymers so we have looked for alternative β-strand donors and acceptors. A potential β-strand donor would be the amino terminus of AGT which is extended by 50 residues compared to other serpins. A possible model for the AGT polymer is shown in Figure 9 in which the N-terminal extension of one molecule anneals as a dissociable strand on the edge of the A-sheet of another to give an s7A linkage similar to

that of native PAI-1 [35,43] (Figure 9). The increase in overall β-sheet structure characterized by an aberrant β-strand linkage is consistent with the 215 nm minimum of the AGT polymer far-UV spectrum (Figure 4). AGT polymers lacked the extreme stability typical of serpin polymers formed through an A-sheet β-strand insertion (Figure 5B). This lower stability is compatible with an additional edge strand forming hydrogen bonds on only one side. The stable closure of the A-sheet seen in AGT would be a necessity for the formation of this s7A linkage. Other features of this model in keeping with our findings are (i) the reactive centre loop remains accessible while the N-terminus is hidden and inaccessible to renin (Figures 6 and 8), (ii) the Cys18-Cys138 disulphide linkage is close enough to Cys232 for a thiol exchange to link adjacent monomers and further inactivate AGT (Figure 2A,B; Figure 3B,C) [29], and (iii) the proximity of N-terminal histidine residues to positively charged residues in Helix F may be prevented by their protonation at acidic pH (Figure 7).

A proportion of *ex vivo* HMrA consists of monomers in which the RCL has been cleaved at the P6-P5 position. Our experiments provide two alternative explanations for the presence of cleaved polymers *in vivo*: either cleaved AGT monomers polymerize or intact AGT monomers polymerize and undergo subsequent proteinase cleavage. Monomeric cleaved AGT is not detectable in human plasma [21] and yet cleaved AGT polymers can be the predominant form [20] which makes the latter the more plausible route.

We have shown that polymerization of AGT can be induced *in vitro* at temperatures above 45 ^{o}C, but obviously this mechanism is not relevant *in vivo*. The presence of destabilizing mutations might enhance polymerization of AGT under physiological conditions, as with other serpins [47]. However, this cannot explain the increased polymerization associated with pregnancy because the primary structure of this protein is unaltered. A microenvironment or a protein partner specific to pregnancy (possibly within the placenta) might reduce the stability of the monomer enough to accelerate polymerization at 37 ^{o}C. Another possibility is that changes in the highly heterogeneous glycosylation pattern of AGT during pregnancy may affect its behaviour. Alternatively, polymerization may occur intracellularly with *de novo* protein in a partially unfolded state. Short chain polymers entering the circulation could then seed AGT polymerization at other sites [34].

The cleavage of AGT by renin is the rate-limiting step in the renin-angiotensin system [6,7]. Polymerization of AGT into HMrA would lead to reduced generation of AngI and AngII, decreased vasoconstriction and a reduction in blood pressure. Polymerization of AGT could therefore occur as a pathological effect, contributing to the low blood pressure and "shock" associated with many severe illnesses. However, since the polymerization of AGT would lead to a reduction in blood pressure, elevated HMrA is also actually an appropriate response to hypertension. Such appropriate polymerization would be unique among serpins to date. Polymerization of many inhibitory serpins has been described, but in all cases it results in a deficiency of the serpin because the polymerized protein is inactive [31,40,48,49]. The ability of AGT to modulate its activity as a renin substrate through polymerization could explain the puzzling evolutionary conservation of a serpin framework in this large protein that apparently functions simply as a peptide donor.

ACKNOWLEDGEMENTS

We wish to thank Ms. Diane Thibeault (BioMega Research Division of Boehringer Ingelheim (Canada) Ltd.) for the gift of recombinant renin, Dr. Duane Tewksbury (Marshfield Medical Research Foundation, USA) for the gift of polyclonal antibody to AGT, Dr. Aiwu Zhou (CIMR, Cambridge) for providing RCL peptides, Dr. Michael Harbour for performing mass spectrometry (Proteomics Facility, MRC Dunn Human Nutrition Unit, Cambridge), and Dr Rosa Streatfeild-James for the angiotensinogen model. We are grateful to Dr. Didier Belorgey and Dr. Aiwu Zhou for helpful discussion in the preparation of this manuscript.

REFERENCES

1. Doolittle, R. F. (1983) Angiotensinogen is related to the antitrypsin-antithrombin-ovalbumin family. Science **222**, 417-419
2. Irving, J. A., Pike, R. N., Lesk, A.M., and Whisstock, J.C. (2000) Phylogeny of the serpin superfamily: implications of patterns of amino acid conservation for structure and function. Genome Res. **10**,1845-1864
3. Stein, P. E., Tewksbury, D. A., and Carrell, R. W. (1989) Ovalbumin and angiotensinogen lack serpin S→R conformational change. Biochem. J. **262**, 103-107
4. Becerra, S. P., Sagasti, A., Spinella, P., and Notario, V. (1995*)* Pigment epithelium-derived factor behaves like a noninhibitory serpin. Neurotrophic activity does not require the serpin reactive loop. J. Biol. Chem. **270**, 25992-25999
5. Pemberton, P. A., Wong, D. T., Gibson, H. L., Kiefer, M. C., Fitzpatrick, P. A., Sager, R., and Barr, P. J. (1995) The tumor suppressor maspin does not undergo the stressed to relaxed transition or inhibit trypsin-like serine proteases. Evidence that maspin is not a protease inhibitory serpin. J. Biol Chem. **270**, 15832-15837
6. Gould, A. B., and Green, D. (1971) Kinetics of the human renin and human substrate reaction. Cardiovasc. Res. **5**, 86-89

7. Skeggs, L. T., Dorer, F. E., Kahn, J. R., Lentz, K. E., and Levine, M. (1976) The biochemistry of the renin-angiotensin system and its role in hypertension. Am. J. Med. **60**, 737-748
8. Lalouel, J. M., Rohrwasser, A., Terreros, D., Morgan, T., and Ward, K. (2001) Angiotensinogen in essential hypertension: from genetics to nephrology. J. Am. Soc. Nephrol. **12**, 606-615
9. Tewksbury, D. A., Frome, W.L., and Dumas, M. L. (1978) Characterization of human angiotensinogen. J. Biol. Chem. **253**, 3817-3820
10. Campbell, C .J., Charlton, P. A., Grinham, C .J., Mooney, C.J., and Pendlebury, J. E. (1987) The rapid purification and partial characterization of human serum angiotensinogen. Biochem. J. **243**, 121-126
11. Gordon, D. B., and Sachin, I. N. (1977) Chromatographic separation of multiple renin substrates in women: effect of pregnancy and oral contraceptives. Proc. Soc. Exp. Biol. Med. **156**, 461-464
12. Tewksbury, D. A., and Dart, R. A. (1982) High molecular weight angiotensinogen levels in hypertensive pregnant women. Hypertension **4**, 729-734
13. Tetlow, H. J., and Broughton-Pipkin, F. (1986) Changing renin substrates in human pregnancy. J. Endocrinol. **109**, 257-262
14. Lenz, T., Sealey, J.E., and Tewksbury, D.A. (1993) Regional distribution of the angiotensinogens in human placentae. Placenta **14**, 695-699
15. Christiansen, M., Jaliashvili, I., Overgaard, M. T., Ensinger, C., Obrist, P., and Oxvig, C. (2000) Quantification and characterization of pregnancy-associated complexes of angiotensinogen and the proform of eosinophil major basic protein in serum and amniotic fluid. Clin. Chem. **46**, 1099-1105
16. Tewksbury, D. A., and Tryon, E. S. (1989) Immunochemical comparison of high molecular weight angiotensinogen from amniotic fluid, plasma of men, and plasma of pregnant women. Am. J. Hypertens. **2**, 411-413
17. Tewksbury, D. A. (1996) Quantitation of five forms of high molecular weight angiotensinogen from human placenta. Am. J. Hypertens. **9**, 1029-1034
18. Ramaha, A., Celerier, J., and Patston, P. A. (2003) Characterization of different high molecular weight angiotensinogen forms. Am. J. Hypertens. **16**, 478-483
19. Tewksbury, D., Frome, W., Kaiser, S., and Vevea, D. (1997) 38. Study of the composition and formation of high molecular weight angiotensinogen. Abstracts of the 12th Scientific Meeting of the Inter-American Society of Hypertension
20. Tewksbury, D. A., Goodman, J. R., Kaiser, S. J., Burrill, R. E., and Brown, H. L. (2000) Quantitation of the five forms of plasma high molecular weight angiotensinogen in women with pregnancy-induced hypertension. Am. J. Hypertens. **13**, 221-225
21. Celerier, J., Schmid, G., Le Caer, J. P., Gimenez-Roqueplo, A. P., Bur, D., Friedlein, A., Langen, H., Corvol, P., and Jeunemaitre, X. (2000) Characterization of a human angiotensinogen cleaved in its reactive center loop by a proteolytic activity from Chinese hamster ovary cells. J. Biol. Chem. **275**, 10648-10654
22. Shionoiri, H., Gotoh, E., Kaneko, Y., Eggena, P., Sambhi, M. P. (1983) Differences in the kinetic rate constants of normal and high molecular weight renin substrate from term pregnancy human plasma. Endocrinol. Jpn. **30**, 731-736
23. Tryon, E. S., and Tewksbury, D. A. (1995) Kinetic analysis of the reaction of human renin with human

high and low molecular weight angiotensinogen. Hypertens. Pregnancy **14**, 327-338

24. Tewksbury, D. A., Premeau, M. R., Dumas, M. L., and Frome, W. L. (1977) Purification of human angiotensinogen. Circ. Res. **41**, 29-33
25. Schagger, H., and von Jagow, G. (1987) Tricine-sodium dodecyl sulfate-polyacrylamide gel electrophoresis for the separation of proteins in the range from 1 to 100 kDa. Anal. Biochem. **166**, 368-379
26. Towbin, H., Staehelin, T., and Gordon, J. (1979) Electrophoretic transfer of proteins from polyacrylamide gels to nitrocellulose sheets: procedure and some applications. Proc. Natl. Acad. Sci. USA. **76**, 4350-4354
27. Dafforn, T. R., Mahadeva, R., Elliott, P. R., Sivasothy, P., and Lomas, D. A. (1999) A kinetic mechanism for the polymerization of α1-antitrypsin. J. Biol. Chem. **274**, 9548-9555
28. Bruch, M., Weiss, V., and Engel, J. (1988) Plasma serine proteinase inhibitors (serpins) exhibit major conformational changes and a large increase in conformational stability upon cleavage at their reactive sites. J. Biol. Chem. **263**, 16626-16630
29. Streatfeild-James, R. M., Williamson, D., Pike, R. N., Tewksbury, D., Carrell, R. W., and Coughlin, P. B. (1998) Angiotensinogen cleavage by renin: importance of a structurally constrained N-terminus. FEBS Lett. **436**, 267-270
30. Lomas, D. A., Finch, J. T., Seyama, K., Nukiwa, T., and Carrell, R. W. (1993) α1-antitrypsin Siiyama (Ser53→Phe). Further evidence for intracellular loop-sheet polymerization. J. Biol. Chem. **268**, 15333-15335
31. Davis, R. L., Shrimpton, A. E., Holohan, P.D., Bradshaw, C., Feiglin, D., Collins, G.H., Sonderegger, P., Kinter, J., Becker, L. M., Lacbawan, F., Krasnewich, D., Muenke, M., Lawrence, D. A., Yerby, M.S., Shaw, C.M., Gooptu, B., Elliott, P. R., Finch, J. T., Carrell, R. W., and Lomas, D.A. (1999) Familial dementia caused by polymerization of mutant neuroserpin. Nature **401**, 376-379
32. Lomas, D. A., Evans, D. L., Finch, J. T., and Carrell, R. W. (1992) The mechanism of Z α1-antitrypsin accumulation in the liver. Nature **357**, 605-607
33. Mahadeva, R., Chang, W. S., Dafforn, T. R., Oakley, D. J., Foreman, R.C., Calvin, J., Wight, D. G., Stein, P. E., and Carrell, R.W. (1995) Heteropolymerization of S, I, and Z α1-antitrypsin and liver cirrhosis. Nat. Struct. Biol. **2**, 96-113
34. Crowther, D.C., Serpell, L.C., Dafforn, T.R., Gooptu, B., and Lomas, D.A. (2003) Nucleation of α1-antichymotrypsin polymerization. Biochemistry **42**, 2355-2363
35. Zhou, A., Faint, R., Charlton, P., Dafforn, T.R., Carrell, R. W., and Lomas, D. A. (2001) Polymerization of plasminogen activator inhibitor-1. J. Biol. Chem. **276**, 9115-9122
36. Sivasothy, P., Dafforn, T. R., Gettins, P. G., and Lomas, D. A. (2000) Pathogenic α1-antitrypsin polymers are formed by reactive loop-β-sheet A linkage. J. Biol. Chem. **275**, 33663-33668
37. Stein, P., and Chothia, C. (1991) Serpin tertiary structure transformation. J. Mol. Biol. **221**, 615-621
38. Lomas, D.A., Elliott, P. R., Chang, W. S., Wardell, M. R., and Carrell, R.W. (1995) Preparation and characterization of latent α1-antitrypsin. J. Biol. Chem. **270**, 5282-5288
39. Elliott, P. R., Lomas, D. A., Carrell, R. W., and Abrahams, J. P. (1996) Inhibitory conformation of the reactive loop of α1-antitrypsin. Nat. Struct. Biol. **3**, 676-681
40. Bruce, D., Perry, D.J., Borg, J. Y., Carrell, R.W., Wardell, M. R. (1994) Thromboembolic disease due to

thermolabile conformational changes of antithrombin Rouen-VI (187 Asn→Asp) J. Clin. Invest. **94**, 2265-2274

41. Carrell, R. W., Stein, P. E., Fermi, G., and Wardell, M.R. (1994) Biological implications of a 3A structure of dimeric antithrombin. Structure **2**, 257-270
42. Lomas, D. A., Elliott, P. R., Sidhar, S. K., Foreman, R. C., Finch, J. T., Cox, D. W., Whisstock, J. C., and Carrell, R. W. (1995) α1-Antitrypsin Mmalton (Phe52Δ) forms loop-sheet polymers *in vivo*. Evidence for the C sheet mechanism of polymerization. J. Biol. Chem. **270**, 16864-16870
43. Sharp, A. M., Stein, P. E., Pannu, N. S., Carrell, R. W., Berkenpas, M. B., Ginsburg, D., Lawrence, D. A., and Read, R. J. (1999) The active conformation of plasminogen activator inhibitor 1, a target for drugs to control fibrinolysis and cell adhesion. Structure Fold Des. **7**, 111-118
44. Schulze, A.J., Baumann, U., Knof, S., Jaeger, E., Huber, R., and Laurell, C. B. (1990) Structural transition of α1-antitrypsin by a peptide sequentially similar to β-strand s4A. Eur. J. Biochem. **194**, 51-56
45. Ramaha, A., and Patston, P. A. (2002) Release and degradation of angiotensin I and angiotensin II from angiotensinogen by neutrophil serine proteinases. Arch. Biochem. Biophys. **397**, 77-83
46. Tewksbury, D. A., Pan, N., and Kaiser, S. J. (2003) Detection of a receptor for angiotensinogen on placental cells. Am. J. Hypertens. **16**, 59-62
47. Carrell, R. W., and Stein, P. E. (1996) The biostructural pathology of the serpins: critical function of sheet opening mechanism. Biol. Chem. Hoppe Seyler. **377**,1-17
48. Lomas, D. A., and Carrell, R.W. (2002) Serpinopathies and the conformational dementias. Nat. Rev. Genet. **3**, 759-768
49. Stein, P. E., and Carrell, R. W. (1995) What do dysfunctional serpins tell us about molecular mobility and disease? Nat. Struct. Biol. **2**, 96-113

FIGURES

Figure 1 Polymerization of AGT under physiological conditions

AGT was incubated at 37 ºC and 0.07 mg/ml in 1 x PBS (i) for 0 to 70 days, (ii) for 24 h containing 0, 2, 4 or 6 M urea, and (iii) for 24 h at 40, 45, 50 or 55 ºC, as indicated. Aliquots were analyzed by 7.5% nondenaturing PAGE and silver staining. Lanes contained 1.4 μg of protein. The positions of monomers (m), dimers (d), trimers (tr) and tetramers (te) are marked with arrows. *Ex vivo* AGT polymers isolated from human plasma are shown (E).

Figure 2 Analysis of AGT polymers by gel electrophoresis and electron microscopy

(A) Polymerization of intact AGT. AGT was incubated at 55 ºC and 0.2 mg/ml in 30 mM sodium phosphate, 150 mM NaCl, 0.5 mM EDTA, pH 7.4 (referred to as buffer). Aliquots taken over time (0 to 45 min and 2 to 54 h) were analyzed by (i) 7.5% nondenaturing PAGE and (ii) 10% nonreducing SDS-PAGE. Lanes contained (i) 4 μg and (ii) 2 μg of protein.

(B) Polymerization of reactive centre loop (RCL)-cleaved AGT (i) Cleavage of AGT by thermolysin. Coomassie staining of a 16% SDS-PAGE of AGT untreated (-) or cleaved in the RCL with thermolysin (+) showing the 4 kDa C-terminal peptide. (ii) and (iii) Heat-induced polymerization of RCL-cleaved AGT. Thermolysin treated AGT was incubated at 55 ^{o}C and 0.2 mg/ml in buffer and aliquots taken over time (0 to 54 h) were analyzed by (ii) 7.5% nondenaturing PAGE and (iii) 10% nonreducing SDS-PAGE. Lanes contained (i) 5 μg and (ii) 4 μg and (iii) 2 μg of protein. (N) Intact native AGT control.

(C) Electron micrographs of AGT polymers (ii) formed by heating (0.5 mg/ml) at 55 ^{o}C for 24 h. Shown in the left hand panel (i) for comparative purposes are polymers formed by heating α1-antitrypsin (0.25 mg/ml) at 65 ^{o}C for 12 h. All preparations were stained negatively with 2% (w/v) uranyl acetate and viewed with a magnification of 57, 000 x. The scale bar represents 100 nm.

Figure 3 Noncovalent and covalent disulphide linkage in AGT polymerization

(A) The disappearance of monomeric AGT during polymerization at 48 ^{o}C at 0.07 mg/ml (**....**), 0.2 mg/ml (**----**) and 0.7 mg/ml (—). (i) Monomeric AGT at time points during a 22 h incubation was quantified relative to the unheated sample (100%) by densitometry of silver stained nondenaturing gels. Results are the average of three experiments. (ii) Nondenaturing PAGE of samples from (i) taken after 22 h (arrowed) (lanes contain 1.4 μg AGT).

(B) The disappearance of monomeric AGT during polymerization on nondenaturing gels (black bars) and nonreducing SDS-PAGE (grey bars) at 55 ^{o}C. Monomeric AGT at different time points during a 54 h incubation was quantified relative to the unheated sample (100%) after densitometry of Coomassie stained gels. Results are the average of three experiments.

(C) Influence of modification of thiol groups in AGT on its polymerization. Polymerization of AGT tested by (i) nondenaturing PAGE (each lane contains 4 μg AGT) and (ii) nonreducing SDS-PAGE (each lane contains 2 μg AGT). AGT (0.2 mg/ml) incubated at 4 ^{o}C (4) or 55 ^{o}C (55) in buffer for 54 h after no treatment (control), reduction with 10 mM dithiothreitol (DTT) or alkylation with 10 mM N-ethylmaleimide (NEM).

Figure 4 Far-ultraviolet CD spectra of intact and RCL-cleaved AGT monomers and polymers

Far-UV CD spectra were measured at 25 ºC for intact (solid line) and RCL-cleaved (dashed line) AGT monomers (A) and polymers (B). Polymers were formed by incubating AGT in buffer at 1.5 mg/ml at 55 ºC for 24 h and were confirmed by nondenaturing PAGE. Before recording, samples were diluted to 0.3 mg/ml in 10 mM sodium phosphate, 50 mM NaCl, pH 7.4. The spectra shown are averages of at least two separately run spectra.

Figure 5 Stability of AGT monomers and polymers

(A) Thermal stability of AGT monomers and polymers. CD signal at 222 nm for monomeric (solid line) and polymeric (dashed line) samples of AGT while increasing temperature at 1 ºC /min. Polymers were formed by incubating AGT in buffer at 1.5 mg/ml at 55 ºC for 24 h. Before recording, samples were diluted to 0.3 mg/ml in 10 mM sodium phosphate, 50 mM NaCl, pH7.4. (B) The urea-induced unfolding of AGT monomers and polymers. Composite gel of 7.5% nondenaturing gel electrophoresis in the presence of 0 M, 2 M, 4 M, 6 M and 8 M urea of AGT monomers (M) and polymers (P) (4 μg protein each lane). AGT polymers formed by heating AGT (0.2 mg /ml) in buffer at 55 ºC for 3 h.

Figure 6 Absence of reactive centre loop-sheet interactions in AGT polymers

Cleavage of monomeric and polymeric AGT with thermolysin. Monomeric and polymeric AGT were incubated in reaction buffer at 37 ºC for 1 h before loading on (i) 10% SDS-PAGE (2 μg protein / lane) and (ii) 7.5% non-denaturing gel (4 μg protein / lane). The ratios of protein:proteinase were (0) no thermolysin, (1) 900:1, (2) 300:1 based on w/w.

Figure 7 pH-dependence of the polymerization of AGT

Following (A) no treatment, (B) histidine modification with 1.0 mM DEPC at 25 ºC for 15 min in 20 mM sodium phosphate, 75 mM NaCl, 1.0 mM EDTA, pH 6.0, (C) reduction with 10 mM dithiothreitol (DTT) at 25 ºC for 2 h in 20 mM sodium phosphate, 75 mM NaCl, 1.0 mM EDTA, pH 7.0, and (D) cleavage by 3.0 nM renin at 37 ºC for 72 h in 30 mM sodium phosphate, 150 mM NaCl, 1.0 mM EDTA, pH 6.0, buffers were adjusted to 150 mM NaCl and pH from 4 to 9 as indicated, and AGT heated at 55 ºC for 1 h. Samples were loaded on 7.5% nondenaturing gels (4 μg protein / lane). (A) to (D), Lane C contains unheated sample of each treated AGT.

Figure 8 Susceptibility of heat-induced polymers of AGT to renin

(A) AGT was incubated at 55 ºC and 0.15 mg/ml in buffer and aliquots taken over time (0 to 18 h). Samples were then incubated in the presence of 1.5 nM renin at 37 ºC for 1 h. Polymerization (black bars) was quantified as in Figure 3B. Released AngI (grey bars). (B) RCL-cleaved AGT was prepared by incubating with thermolysin at a final protein: proteinase ratio of 200:1 (w/w) at 37 ºC for 1 h. Samples of intact and RCL-cleaved AGT were incubated at 4 ºC (monomer) or 55 ºC (polymer) and 0.3 mg/ml in buffer for 3 h and then incubated in the presence of 0.5 nM renin at 37 ºC for 0 to 8 h. Intact polymer (—), cleaved polymer (**.....**), intact monomer (----), cleaved monomer (– – – –).

Samples were loaded onto 10% reducing SDS-PAGE, transferred to PVDF membrane, and developed with (i) α-AGT and (ii) α-AngI antibodies. Bands were quantified relative to total AGT and to samples not treated with renin (0% AngI release; 100% AngI retained) after densitometry. Results are the average of three experiments.

Figure 9 Proposed model of an AGT s7A loop-sheet dimer

Our dimer model was built from a model of the AGT monomer [29] based on sequence alignment with ovalbumin. This model does not include the 69 N-terminal amino acids of AGT, which are illustrated by a dotted line. The disulphide bond between Cys18 and Cys138 and the position of the reactive centre loop (RCL) are indicated. A. Side view of the proposed AGT dimer showing how the N-terminus of AGT would be hidden and inaccessible to renin. The proximity of Cys138 and Cys232 is evident. B. View rotated 90 º showing how the N-terminal extension of an AGT monomer could be positioned to form a new strand against the edge of β-sheet A of a second monomer. The position of Cys232 adjacent to Helix F is indicated (●).

Biochemical Journal Immediate Publication. Published on 27 Jul 2006 as manuscript BJ20060444

Figure 1

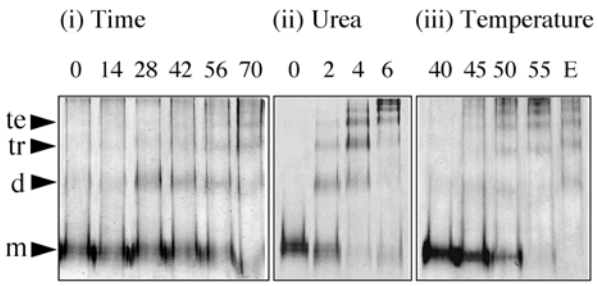

Biochemical Journal Immediate Publication. Published on 27 Jul 2006 as manuscript BJ20060444

Figure 2

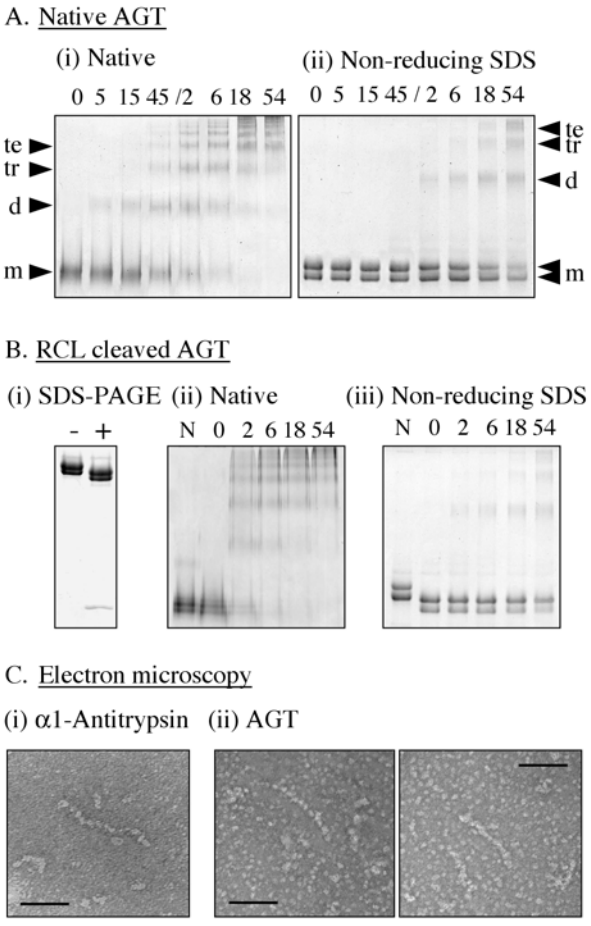

Biochemical Journal Immediate Publication. Published on 27 Jul 2006 as manuscript BJ20060444

Figure 3

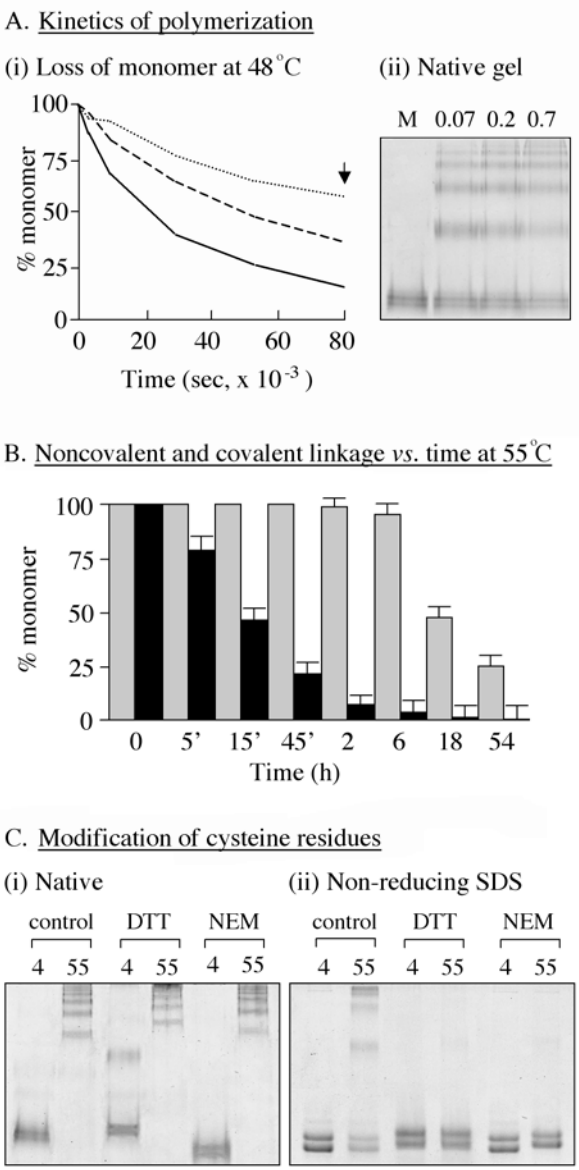

Biochemical Journal Immediate Publication. Published on 27 Jul 2006 as manuscript BJ20060444

Figure 4

A. Far-UV CD spectra of AGT monomers

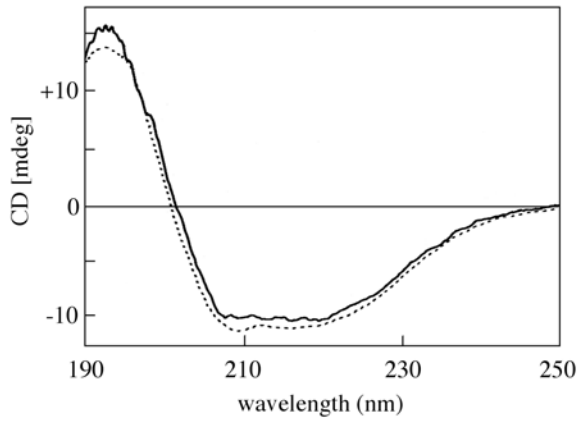

B. Far-UV CD spectra of AGT polymers

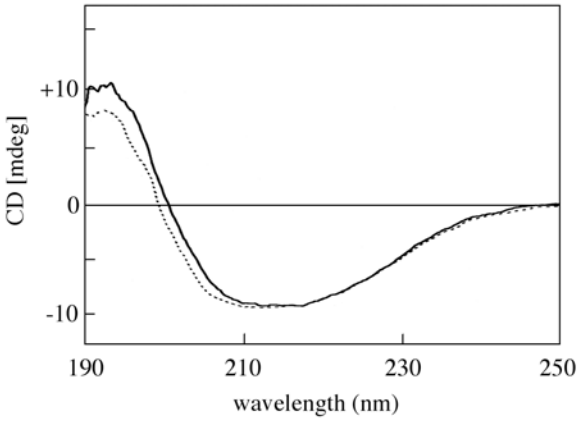

Biochemical Journal Immediate Publication. Published on 27 Jul 2006 as manuscript BJ20060444

Figure 5

A. Stability to heat

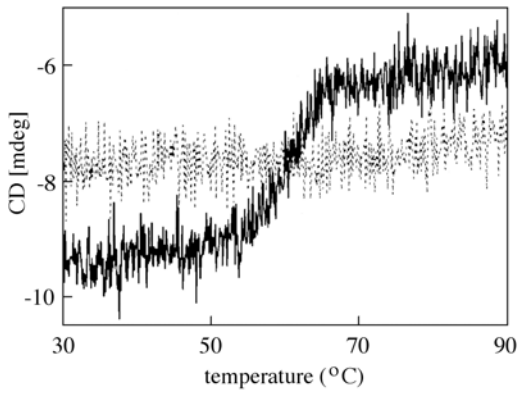

B. Stability to urea

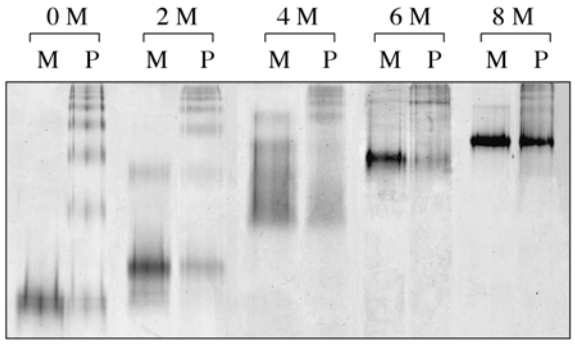

Biochemical Journal Immediate Publication. Published on 27 Jul 2006 as manuscript BJ20060444

Figure 6

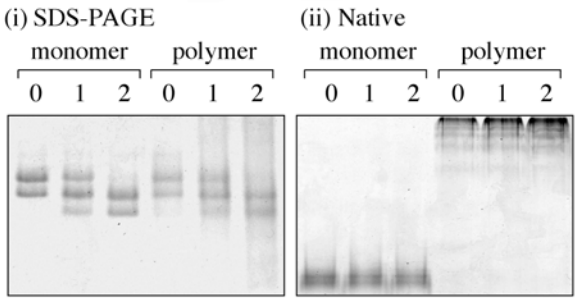

Biochemical Journal Immediate Publication. Published on 27 Jul 2006 as manuscript BJ20060444

Figure 7

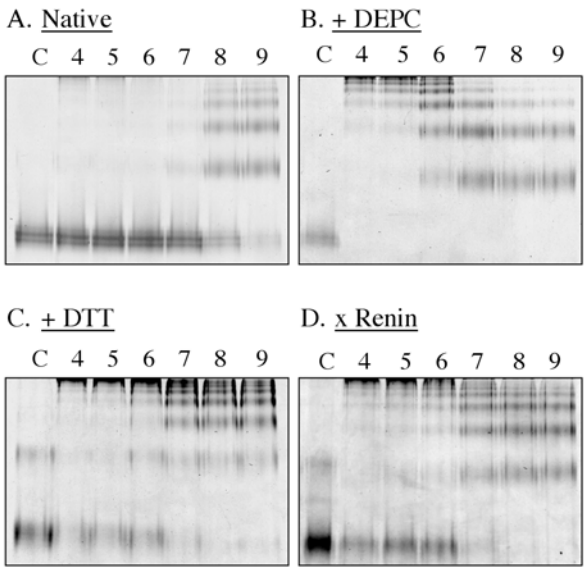

Biochemical Journal Immediate Publication. Published on 27 Jul 2006 as manuscript BJ20060444

Figure 8

A. Angiotensin I release *vs.* polymerization

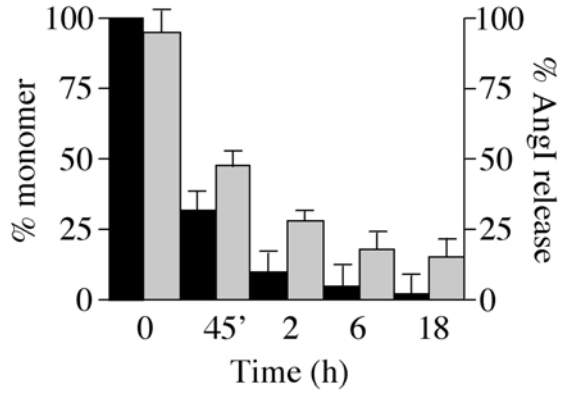

B. Retention of AngI on monomer and polymer

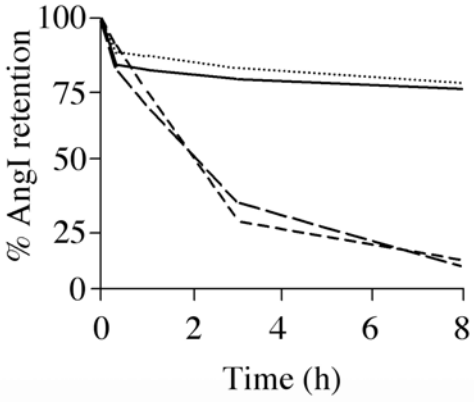

Biochemical Journal Immediate Publication. Published on 27 Jul 2006 as manuscript BJ20060444

Figure 9